RIS-Assisted Grant-Free NOMA

Recep Akif Tasci*, Fatih Kilinc*, Abdulkadir Celik•, Asmaa Abdallah•, Ahmed M. Eltawil• and Ertugrul Basar*

*Communications Research and Innovation Laboratory (CoreLab),
Department of Electrical and Electronics Engineering, Koç University, Sariyer 34450, Istanbul, Turkey.
•Computer, Electrical, and Mathematical Sciences & Engineering (CEMSE) Division,
King Abdullah University of Science and Technology (KAUST), Thuwal, KSA 23955-6900

Abstract—This paper introduces a reconfigurable intelligent surface (RIS)-assisted grant-free non-orthogonal multiple access (GF-NOMA) scheme. To ensure the power reception disparity required by the power domain NOMA (PD-NOMA), we propose a joint user clustering and RIS assignment/alignment approach that maximizes the network sum rate by judiciously pairing user equipments (UEs) with distinct channel gains, assigning RISs to proper clusters, and aligning RIS phase shifts to the cluster members yielding the highest cluster sum rate. Once UEs are acknowledged with the cluster index, they are allowed to access their resource blocks (RBs) at any time requiring neither further grant acquisitions from the base station (BS) nor power control as all UEs are requested to transmit at the same power. In this way, the proposed approach performs an implicit over-the-air power control with minimal control signaling between the BS and UEs, which has shown to deliver up to 20% higher network sum rate than benchmark GF-NOMA and grant-based optimal (OPT) PD-NOMA schemes depending on the network parameters. The given numerical results also investigate the impact of UE density, RIS deployment, and RIS hardware specifications on the overall performance of the proposed RIS-aided GF-NOMA scheme.

Index Terms—Reconfigurable intelligent surface, power domain, grant-free, non-orthogonal multiple access, clustering, resource allocation.

I. INTRODUCTION

Reconfigurable intelligent surfaces (RISs) have emerged as a transformative technology envisioned for next-generation wireless networks to improve the spectral efficiency (SE) with low power consumption and hardware costs [1]. RISs have low-cost and low-power hardware as they consist of a large number of passive elements. The RIS controller manipulates the reflection of incident electromagnetic waves towards the desired direction by intelligently controlling the phase shift of elements [2]. The passive beamforming nature of RISs has been shown to improve network capacity [1], [2], enhance the end-to-end performance of multi-hop communications [3], and deliver a performance comparable to traditional relaying schemes [4].

Moreover, non-orthogonal multiple access (NOMA) has also been recognized as a promising candidate to enable massive machine-type communication by multiplexing several user equipments (UEs) on the same network resources [5], [6]. In particular, power domain NOMA (PD-NOMA) improves the SE by multiplexing UEs with different channel gain and controlling transmit power such that successive interference

cancellation (SIC) can be performed at the receiver. As the network size increases, PD-NOMA starts suffering from power control complexity, user pairing and resource allocation overhead, and ramifications of channel state information (CSI) acquisition [7]. NOMA has also been investigated with emerging technologies such as index modulation [8], cognitive radios [9], and unmanned aerial vehicles-aided wireless networks [10]. Recently, RISs have received attention thanks to their ability to create the reception power disparity required by PD-NOMA. While the RIS-aided NOMA is analyzed in [11], dynamic and static RIS configurations for multi-user NOMA schemes are considered in [12]. The authors of [13] studied partitioning of RIS to facilitate PD-NOMA. Despite the fact that all of the aforementioned systems are grant-based (GB), there is still an urgent need to address the signaling overhead and computational complexity issues that are a bottleneck for NOMA technology. This is why there has lately been a lot of interest in the study of grant-free NOMA (GF-NOMA) schemes that UEs can operate without grant acquisition. The purpose of the PD GF-NOMA scheme is to eliminate the need of the complex power control operation, where the UEs can instead use fixed powers and rely on the channel gains disparity which leads to implicit over-the-air power control and reception power disparity. Multiple access based [7], compute and forward based, compressing sensing based [14], index modulation based [15], and the transmit power pool based [16] GF-NOMA schemes are studied in the literature. ALOHA-NOMA schemes [17] and semi GF-NOMA scheme where the GB and GF users share the same spectrum is proposed in [18]. As pointed out by a recent survey on GF-NOMA, RIS-aided GF-NOMA is a promising technology but has not been explored in-depth yet [7]. To the best of the authors' knowledge, RIS-aided GF-NOMA is considered only in [19], where authors propose a semi GF-NOMA by using deep reinforcement learning to control power and phase shifts.

In this paper, we propose an RIS-aided GF-NOMA scheme based on a novel joint user clustering and RIS assignment/alignment mechanism. Once UEs are acknowledged with a cluster index, they are allowed to access their RBs at any time requiring neither further grant acquisitions from the BS nor power control as all UEs are requested to transmit at the same power. The required power disparity is obtained by three levels of implicit power control: 1) by clustering UEs with different channel gains into the same cluster, 2) properly assigning RISs to clusters to increase power reception disparity, and 3) aligning the phase shift matrix of RIS to

the cluster members giving the highest possible cluster sum rate. In this way, the proposed approach performs over-the-air power control by judiciously pairing UEs, assigning RISs, and aligning phase shifts of RISs. Since this joint combinatorial problem is known to be NP-Hard, we develop an iterative 3D assignment approach that forms clusters and assigns/aligns RISs to maximize the network sum rate. The proposed scheme has shown to outperform GB optimal (OPT) PD-NOMA and GF-NOMA schemes.

The rest of this paper can be summarized as follows. In Section II, we present the considered network and channel model, the proposed signal model and the RIS phase alignment process. In Section III, we discuss the problem formulation and explain the proposed solution methodology, and present the proposed iterative 3D clustering approach in Section III-B. Finally, in Section IV, we present numerical results and the paper is concluded in Section V.

II. NETWORK MODEL

We consider uplink (UL) operation of a network consisting of a single BS serving U UEs over R RBs with W [Hz] bandwidth, whose sets are denoted by $\mathcal{U}$ and $\mathcal{R}$, respectively. All UEs operate at an identical power, p_{id}, which is broadcast by the BS over a control channel. Without loss of generality, UEs are assumed to be uniformly distributed over a cell area of radius D. To show proposed GF-NOMA schemes suitability for massive connectivity, we consider a dense network scenario (i.e., $U \gg R$) and group multiple UEs to utilize a single resource block. That is, the number of clusters C is the same with R, and RB/cluster terms are used interchangeably throughout the paper. Even though R and C are fixed, U can dynamically change according to spatio-temporal characteristics of the network traffic. Hence, the maximum cluster size is set as $K = \lceil \frac{U}{R} \rceil$. Accordingly, the cluster set utilizing RB_r is defined by $\mathcal{C}_r = \{UE_u \mid \chi_r^u = 1, \forall u \in \mathcal{U}, \sum_{u \in \mathcal{U}} \chi_r^u \leq K\}$, where χ_r^u is the binary indicator, $\chi_r^u = 1$ if UE_u belongs to rth cluster, otherwise $\chi_r^u = 0$.

In order to improve network performance and facilitate the GF-NOMA, M RISs are uniformly deployed in a disk having inner and outer radius of D_{in} and D_{out}, where D_{in} ensures that RISs are placed at the far-field of the BS as shown in Fig. 1 and $D_{\text{in}} \leq D_{\text{out}} \leq D$. Each physical RIS is partitioned into G logical sub-blocks, each with N elements, resulting in an overall $B = MG$ RIS blocks. Each block can be exploited by a member of a cluster, and a cluster cannot be assigned to more than one block. Accordingly, the set of RIS blocks are denoted by $\mathcal{B}$, and the bth RIS block is denoted by RIS_b. The binary RIS assignment matrix is denoted by $\mathbf{\Delta} \in \{0,1\}^{B \times U \times R}$ with entries $\delta_{r,b}^u$ such that $\delta_{r,b}^u = 1$ if RIS_b is assigned to the rth cluster and configured based on the channels of $\text{UE}_u \in \mathcal{C}_r$, $\delta_{r,b}^u = 0$ otherwise. Fig. 1 demonstrates the considered network model where the users in a cluster are shown with the circles in the shades of blue, the RIS assisting the cluster with the blue square, the base station with a black star, the other users in the network with gray circles and the other RISs with green squares assuming there are three users in a cluster. With the
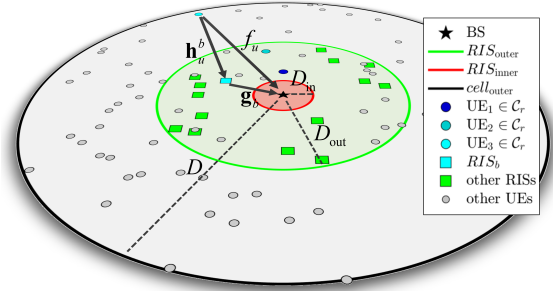
Fig. 1: Network model

help of the 3D clustering algorithm, which will be explained in the next section, we will jointly form the RIS assignment matrix and assign users to clusters according to the modified received power of the users to maximize the sum rate.

The channels are modeled according to the Urban Macro (UMa) scenario of the 3GPP standard specified for 0.5-100 GHz bands [20]. The channel between UE_u and RIS_b is denoted by $\mathbf{h}_u^b = \left[h_{u,b}^1, \ldots, h_{u,b}^n, \ldots, h_{u,b}^N\right] \in \mathbb{C}^{N \times 1}$, where $h_{u,b}^n$ is the channel coefficient from UE_u to nth reflecting element of the RIS_b, $n \in [1, N]$. Similarly, the channel vector between the BS and RIS_b is denoted by $\mathbf{g}_b = \left[g_b^1, \ldots, g_b^n, \ldots, g_b^N\right] \in \mathbb{C}^{N \times 1}$, where g_b^n is the channel coefficient between the BS and nth reflecting element of the RIS_b, $n \in [1, N]$. Moreover, the direct channel from UE_u to the BS is denoted by $f_u \in \mathbb{C}^{1 \times 1}$. All these channels can experience Rayleigh and Rician fading under line-of-sight (LoS) and non-line-of-sight (NLoS) conditions, respectively. The channel coefficients are modeled as

$$h_{u,b}^n = \sqrt{\frac{1}{\lambda_h}} \left(\sqrt{\frac{K_h}{K_h + 1}} h_{u,b}^{n,\text{LoS}} + \sqrt{\frac{1}{K_h + 1}} h_{u,b}^{n,\text{NLoS}} \right), \quad (1)$$

$$g_b^n = \sqrt{\frac{1}{\lambda_g}} \left(\sqrt{\frac{K_g}{K_g + 1}} g_b^{n,\text{LoS}} + \sqrt{\frac{1}{K_g + 1}} g_b^{n,\text{NLoS}} \right), \quad (2)$$

$$f_u = \sqrt{\frac{1}{\lambda_f}} \left(\sqrt{\frac{K_f}{K_f + 1}} f_u^{\text{LoS}} + \sqrt{\frac{1}{K_f + 1}} f_u^{\text{NLoS}} \right), \quad (3)$$

where $K_h/K_g/K_f$ is the Rician factor for $\mathbf{h}_u^b/\mathbf{g}_b/f_u$; $\lambda_h/\lambda_g/\lambda_f$ is the path loss over $\mathbf{h}_u^b/\mathbf{g}_b/f_u$; $h_{u,b}^{n,\text{LoS}}/g_b^{n,\text{LoS}}/f_u^{\text{LoS}}$ is the LoS component and $h_{u,b}^{n,\text{NLoS}}/g_b^{n,\text{NLoS}}/ f_u^{\text{NLoS}} \sim \mathcal{CN}(0,1)$ is the NLoS component of $\mathbf{h}_u^b/\mathbf{g}_b/f_u$. If a channel does not include a LoS component, which mostly refers to Rayleigh fading, we consider the corresponding Rician factor as 0. λ_h, λ_g and λ_f are calculated according to the UMa scenario of the 3GPP standard considering the LoS probability specified in [20].

Based on UE-RIS-BS cascaded channels and UE-BS channels defined in (1)-(3), the received complex baseband signal at the BS over RB_r can be expressed as

$$y_r(\mathbf{\Delta}) = \sqrt{p_{\text{id}}} \left(\sum_{\forall u \in \mathcal{C}_r} \sum_{\forall k,l,m} \underbrace{\mathbf{g}_l^{\text{T}} \left(\mathbf{\Phi}_{k,l}^m \delta_{k,l}^m \right) \mathbf{h}_u^l s_u}_{\text{UEs-RIS-BS}} + \underbrace{f_u s_u}_{\text{UEs-BS}} \right) + n, \quad (4)$$

where $k \in \mathcal{R}$; $l \in \mathcal{B}$; $m \in \mathcal{U}$; $y_r(\mathbf{\Delta})$ is the received signal from members of $\mathcal{C}_r$ at RB$_r$; s_u is the symbol transmitted by UE$_u \in \mathcal{C}_r$; $n \sim \mathcal{CN}(0, \sigma^2)$ is the additive white Gaussian noise with variance $\sigma^2 = N_0 W$; N_0 is the thermal noise power spectral density; $\mathbf{\Phi}_{k,l}^m = \text{diag}\left(\left[\phi_{k,l}^{m,1}, \ldots, \phi_{k,l}^{m,n}, \ldots, \phi_{k,l}^{m,N}\right]\right) \in \mathbb{C}^{N \times N}$ is the phase shift matrix of RIS$_l$ assigned to UE$_m \in \mathcal{C}_k$; and $\phi_{k,l}^{m,n}$ is the phase shift of the nth element of the RIS$_l$ configured as per UE$_m \in \mathcal{C}_k$. Assuming the CSI is acquired through accurate channel estimation methods [21] and $\delta_{k,l}^m = 1$, the phase shifts of RIS$_b$ are configured as per the channel characteristics of UE$_m \in \mathcal{C}_k$

$$\phi_{k,l}^{m,n} = e^{j\angle f_m} e^{-j\angle g_l^n} e^{-j\angle h_{m,l}^n}, \tag{5}$$

where $\angle \cdot$ denotes the phase of complex numbers and element phases cancels the overall channel phases incurred from UE-RIS-BS cascaded channel and UE-BS direct channel.

The SIC receiver at the BS iteratively decodes $y_r(\mathbf{\Delta})$ in the descending order of received signal power. That is, the cluster member with the strongest/weakest reception power is decoded first/last such that the strongest/weakest cluster member observes all/no intra-cluster interference from other cluster members. Correspondingly, $\widetilde{\mathcal{C}}_r$ denotes the cluster set when index set of the users is sorted in descending order according to the received signal power of the users. Accordingly, following from (4), the SINR of ith ordered UE$_u \in \widetilde{\mathcal{C}}_r$ is given by

$$\gamma_{r_{\text{pas}}}^u(\mathbf{\Delta}) = \frac{p_{\text{id}}\left(\sum\limits_{\forall k,l,m} \left|\mathbf{g}_l^{\text{T}}\left(\mathbf{\Phi}_{k,l}^m \delta_{k,l}^m\right)\mathbf{h}_u^l\right|^2 + |f_u|^2\right)}{p_{\text{id}}\left(\sum\limits_{\substack{\forall z \in \widetilde{\mathcal{C}}_r[j>i], \\ \forall k,l,m}} \left|\mathbf{g}_l^{\text{T}}\left(\mathbf{\Phi}_{k,l}^m \delta_{k,l}^m\right)\mathbf{h}_z^l\right|^2 + |f_z|^2\right) + \sigma^2}, \tag{6}$$

where j corresponds to the index of the users with lower received signal power than ith ordered user. Even though the SINR expression in (6) accounts for $s_u, \forall u \in \mathcal{C}_r$ reflected from RIS$_b, \forall b \in \mathcal{B}$, regardless of their assignment, the non-coherent signals reflected from RIS blocks assigned to other clusters have a negligible impact on the received signal from $\mathcal{C}_r$, $y_r(\mathbf{\Delta})$. Accordingly, (6) can be simplified by merely considering the signal reflected from RIS$_b$ assigned to $\mathcal{C}_r$ as follows:

$$\gamma_{r_{\text{pas}}}^u(\mathbf{\Delta}) = \frac{p_{\text{id}}\left(\sum\limits_{\forall m} \left|\mathbf{g}_b^{\text{T}}\left(\mathbf{\Phi}_{r,b}^m \delta_{r,b}^m\right)\mathbf{h}_u^b\right|^2 + |f_u|^2\right)}{p_{\text{id}}\left(\sum\limits_{\substack{\forall z \in \widetilde{\mathcal{C}}_r[j>i], \\ \forall m}} \left|\mathbf{g}_b^{\text{T}}\left(\mathbf{\Phi}_{r,b}^m \delta_{r,b}^m\right)\mathbf{h}_z^b\right|^2 + |f_z|^2\right) + \sigma_{\text{Rx}}^2}. \tag{7}$$

III. RIS ASSISTED GRANT FREE NOMA SCHEME

In this section, we first provide a formal problem formulation, then outline the proposed solution methodology.

A. Problem Definition

The joint user clustering and RIS assignment problem that maximizes overall network sum rate can be formulated as follows:

$$\mathbf{P_1} : \max_{\mathcal{X}, \mathbf{\Delta}} \quad \sum_{\forall r \in \mathcal{R}} \sum_{\forall u \in \mathcal{U}} W \log_2(1 + \chi_r^u \gamma_r^u(\mathbf{\Delta}))$$

s.t.

$$
\begin{aligned}
&\text{C}_1: && \gamma_r^u \geq 2^{q_u/B} - 1, \ \forall u \in \mathcal{C}_r, \forall r \in \mathcal{R}, \\
&\text{C}_2: && \sum_{r \in \mathcal{R}} \chi_r^u = 1, \ \forall u \in \mathcal{U}, \\
&\text{C}_3: && \sum_{\forall u \in \mathcal{U}} \chi_r^u \leq K, \quad \forall r \in \mathcal{R}, \\
&\text{C}_4: && \delta_{r,b}^u \leq \chi_r^u, \quad \forall r \in \mathcal{R}, \forall b \in \mathcal{B}, \forall u \in \mathcal{U}, \\
&\text{C}_5: && \sum_{\forall u \in \mathcal{U}} \sum_{\forall b \in \mathcal{B}} \chi_r^u \delta_{r,b}^u \leq 1, \quad \forall r \in \mathcal{R}, \\
&\text{C}_6: && \sum_{\forall u \in \mathcal{U}} \sum_{\forall r \in \mathcal{R}} \sum_{\forall b \in \mathcal{B}} \delta_{r,b}^u \leq B, \\
&\text{C}_7: && \chi_r^u \in \{0,1\}, \delta_{r,b}^u \in \{0,1\}, \forall r, \forall u, \forall b.
\end{aligned}
\tag{8}
$$

Here, γ_r^u is the signal-to-noise-plus-interference-ratio (SINR) of UE$_u \in \mathcal{C}_r$, $\mathcal{X} \in \{0,1\}^{U \times R}$ is the binary UE clustering matrix with entries χ_r^u. In $\mathbf{P_1}$, C$_1$ ensures that UE$_u$ is satisfied with the quality of service demand q_u [bps] $\forall u \in \mathcal{C}_r, \forall r \in \mathcal{R}$, C$_2$ assures each UE is admitted to a cluster, C$_3$ limits the cluster size by $K = \lceil U/R \rceil$, C$_4$ states that RIS$_b$ cannot be configured as per UE$_u$ if it is not a member of $\mathcal{C}_r$, C$_5$ guarantees each cluster is assisted by at most one RIS block, C$_6$ limits the total RIS assignments by the total number of RIS blocks, and C$_7$ specifies the domain and bounds on optimization variables. $\mathbf{P_1}$ is a mixed integer nonlinear programming (MINLP) problem, which is non-convex due to the interference terms in the SINR expression defined in the next section. Finding an optimal solution to this NP-Hard problem is computationally prohibitive even for a moderate size of network. This necessitates a heuristic solution for real-life implementation, which is discussed next.

B. Proposed Iterative User Clustering and RIS Assignment

The proposed RIS-assisted GF-NOMA scheme allows UEs to access RBs at any time, requiring neither grant acquisition from the BS nor power control at the UE side. Instead, the power disparity requirement of GB PD-NOMA is satisfied by user clustering and RIS assignment through a three-level implicit power control:

1) The first level of power control is obtained by pairing users with different channel gains on the same cluster/RB. Even if UEs operate at identical transmit power, the channel gain disparity introduces a reception power disparity to achieve a higher PD-NOMA gain.

2) The second level of power control is obtained by assigning a proper RIS block to a cluster. It is worth noting that RIS improves overall communication performance if it is deployed near the UE or the BS [3]. Therefore, RIS block assignment plays a crucial role in increasing

the power reception disparity for an improved cluster sum rate.

3) The final level of power control is obtained by selecting the cluster member according to which assigned RIS is configured. Since reception power levels determine the SIC decoding order, the cluster member selection is also critical to improve the overall cluster sum rate.

Before delving into the details of the proposed RIS-assisted GF-NOMA scheme, it is worth reminding that the GB optimal PD-NOMA scheme requires UEs with stronger channels to transmit at the higher powers to maximize the UL-NOMA cluster sum rate [22]. However, this approach is not fair in energy consumption and may result in reduced network lifetime, which is paramount for low-power machine-type communications. Alternatively, the proposed approach improves network lifetime by requiring all UEs to transmit at identical power fairly and constitutes the required power disparity through iterative user clustering and RIS assignment summarized in Algorithm 1. Following cluster initialization, the proposed iterative approach admits a single UE to each cluster at each iteration until all UEs are admitted to a cluster. To this aim, the admissions are determined based on a three-dimensional axial assignment (3D-AA) that yields the maximum network sum rate. The 3D-AA is known to be an NP-Hard problem, whose matching theory-based approximate solutions can obtain results for a square cost matrix with complexity $\mathcal{O}\left(3MV^3\right)$ where M is the number of relaxations and V is the largest dimension of the cost matrix [23].

Algorithm 1 starts with receiving sounding reference signals (SRS), which is a Zadoff-Chu sequence transmitted by each UE separately from the Physical UL shared channel (PUSCH) and physical uplink control channel (PUCCH). UEs can transmit SRS on any subcarriers in the last symbol of an uplink subframe regardless of subcarriers assignments. We especially focus on time-division duplexing (TDD) mode for the sake of channel reciprocity such that SRS may also be sent in the last two symbols of the special subframe if UL pilot time slot (UpPTS) is configured to be in the long format. The SRS is imperative to estimate cascaded and direct channels [21] to determine RIS assignment and configure phase shift matrices accordingly. Notice that the CSI acquisition is an inherent part any communication standard and not specific to the proposed approach. After the cluster size is determined based on the available number of RBs in Line 3, the maximum cluster size is determined in Line 4 based on the UE density. For the sake of cluster initialization, the users are sorted in the descending order of received signal strength of SRS signals in Line 5. Then, the clusters are initialized by admitting the first R users into C clusters in Line 6. Then, the iterative user admission and RIS assignment start in Line 8 where one more user is admitted to each cluster in each iteration. Therefore, the first line of for loop, Line 9, updates the set of UEs awaiting cluster admission, which is denoted by $\mathcal{A}_k$.

To execute 3D-AA, Line 10 calls cost matrix generation procedure given between Line 17 and Line 34, where cost matrix $\boldsymbol{Q} \in \mathbb{R}^{R \times A \times B}$ and temporary RIS alignment matrix

---

Algorithm 1 : Joint UE Clustering and RIS Assignment

1: **Input:** $\mathcal{R}, \mathcal{U}, \mathcal{B}, \mathrm{P}$
2: $\mathbf{h}_u^b / \mathbf{g}_b / f_u \leftarrow$ *Acquire CSI from SRS sent by $UE_u, \forall u \in \mathcal{U}, \forall b \in \mathcal{B}$*
3: $C \leftarrow R$ // *Determine number of clusters*
4: $K \leftarrow \left\lceil \frac{U}{R} \right\rceil$ // *Determine maximum cluster size*
5: $\tilde{\mathcal{U}} \leftarrow \text{SORTDESCEND}(\mathfrak{R}\mathfrak{ss}, \forall u)$ // *UE ordering based on RSS of SRS*
6: $\mathcal{C}_r \leftarrow \tilde{\mathcal{U}}\{r\}, r \in [1, \dots, R]$ // *Initialize clusters*
7: $\chi_r^u \leftarrow 1, u \in \mathcal{C}_r$ //*Initialize UE clustering matrix*
8: **for** $k = 1 : K-1$ **do** // *Iterative UE admission and RIS Assignment starts*
9:     $\mathcal{A}_k \leftarrow \tilde{\mathcal{U}} - \bigcup_{r=1}^{R} \mathcal{C}_r$ // *Initialize admission awaiting UEs*
10:     $\boldsymbol{Q_k}, \boldsymbol{I_k} \leftarrow \text{COST MATRIX}(\boldsymbol{C}_r, \mathcal{A}_k, \mathcal{B})$ // *Generating cost matrix*
11:     $\boldsymbol{Y}_k \leftarrow \text{3D-AXIAL ASSIGNMENT}(\boldsymbol{Q_k}, \mathcal{A}_k)$
12:     $\mathcal{C}_r \leftarrow \mathcal{C}_r \bigcup \mathcal{A}_k\{u\}, y_{r,b}^u = 1, \forall(r, u, b)$ // *Update clusters*
13:     $\chi_{r'}^u \leftarrow 1, u \in \mathcal{C}_r$ // *Update UE clustering matrix*
14:     $\delta_{r,b}^u \leftarrow 1$ iff $u' = \iota_{r,b}^u, u \in \mathcal{C}_r, \forall(r, b)$ //*Update RIS assignments*
15: **end for**
16: **return** $\boldsymbol{\mathcal{X}}, \boldsymbol{\Delta}$

17: **procedure** COST MATRIX$(\boldsymbol{C}_r, \mathcal{A}_k, \mathcal{B})$
18:     $\boldsymbol{Q}, \boldsymbol{I} \leftarrow \boldsymbol{0}^{R \times A \times B}$ // *Initialize $\boldsymbol{Q}$ and $\boldsymbol{I}$ to matrix of zeros*
19:     **for** $r = 1 : \mathcal{R}$ **do**
20:        **for** $b = 1 : B$ **do**
21:           **for** $u = 1 : A$ **do**
22:              $\mathcal{T}_r \leftarrow \mathcal{C}_r \bigcup \mathcal{A}_k\{u\}$ // *Temp. admit u^{th} UE of $\mathcal{A}_k$ to $\mathcal{C}_r$*
23:              **for** $j \in \mathcal{T}_r$ **do**
24:                 $\boldsymbol{\Phi}_{r,b}^j \leftarrow$ Align RIS_b to $\text{UE}_{\mathcal{T}_r\{j\}}$ as per (5)
25:                 $\gamma_r^j \leftarrow$ Obtain SINR as per (7)
26:                 $\eta_j^\star \leftarrow \sum_{j \in \mathcal{T}_r} W \log_2(1 + \gamma_r^j)$
27:              **end for**
28:              $q_{r,b}^u \leftarrow \max(\eta_j^\star, j \in \mathcal{T}_r)$ // *Update cost matrix entries*
29:              $\iota_{r,b}^u \leftarrow \arg\max(\eta_j^\star, j \in \mathcal{T}_r)$ // *Update $\boldsymbol{I}$ entries*
30:           **end for**
31:        **end for**
32:     **end for**
33:     **return** Q, I
34: **end procedure**

35: **procedure** 3D-AXIAL ASSIGNMENT$(\boldsymbol{Q}, \mathcal{A}_k)$
36:     $\overset{\star}{\boldsymbol{Y}} \leftarrow \max_{\boldsymbol{Y}} \sum_{r \in \mathcal{R}} \sum_{b \in \mathcal{B}} \sum_{u \in \mathcal{U}} q_{r,b}^u y_{r,b}^u$
37:        s.t. $\sum_{r \in \mathcal{R}} \sum_{b \in \mathcal{B}} y_{r,b}^u = 1, \forall u \in \mathcal{A}_k$
38:               $\sum_{r \in \mathcal{R}} \sum_{u \in \mathcal{U}} y_{r,b}^u = 1, \forall b \in \mathcal{B}$
39:               $\sum_{b \in \mathcal{R}} \sum_{u \in \mathcal{U}} y_{r,b}^u = 1, \forall r \in \mathcal{R}$
40: **return** $\overset{\star}{\boldsymbol{Y}}$
41: **end procedure**

$\boldsymbol{I} \in \mathbb{N}^{R \times A \times B}$ are formed over three nested for loops. In Line 22, the u-th element of admission awaiting user set is temporarily admitted to $\mathcal{C}_r$, where A denotes the length of the set $\mathcal{A}_k$. Then, the most inner loop between Line 23 and Line 27 determines the cluster member giving the maximum cluster sum rate if RIS_b is aligned as per its channel conditions. To this aim, Line 24 adjusts the phase shift matrix of RIS_b to $\text{UE}_{\mathcal{T}_r\{j\}}$, Line 25 calculates the cluster members' SINR based on adjusted the phase shift matrix as per (7), and finally Line 26 records the cluster sum rate of $\mathcal{T}_r$ if RIS_b is aligned to its j-th member, $\eta_j^\star$. Accordingly, the cost matrix element $q_{r,u}^b$ is updated in Line 28 based on the user cluster member giving the highest possible cluster rate if the phase shift matrix of RIS_b is aligned to itself, whose index matrix (representing the user index) is also stored in a temporary RIS alignment matrix in Line 29.

Following the generation of the cost-matrix, Line 11 calls 3D-AXIAL ASSIGNMENT to find joint user clustering and RIS assignment at k-th iteration. For instance, when 3D-AA returns

$y_{3,4}^5 = 1$, it means that: 1) $UE_{\mathcal{A}_k\{5\}}$ is admitted to $\mathcal{C}_3$, 2) RIS_4 is assigned to $\mathcal{C}_3$, and 3) phase shift matrix of RIS_4 is aligned to assisted user $UE_{u'}$ whose user index stored in $u' = \iota_{3,4}^5$. Thereafter, the cluster members are updated as per the outcome of 3D-AA in Line 12, which is followed by update of user clustering matrix $\mathcal{X}$ and RIS assignment matrix Δ in Line 13 and 14, respectively. The final user clustering and RIS assignment matrices are returned at the end of $(K-1)$-th iteration. Notice in Line 14 that the phase alignment is obtained from the RIS alignment matrix I returned by the COST MATRIX procedure.

The time complexity of the proposed solution is mainly driven by COST MATRIX and 3D-AXIAL ASSIGNMENT procedures. While the complexity of cost matrix computation is $\mathcal{O}\left(\sum_{k=1}^{K-1} RA_k B\right)$ and the time complexity of the 3D-AA is $\mathcal{O}\left(3M\sum_{k=1}^{K-1}(V_k)^3\right)$, where $V_k = \max(R, A_k, B)$. Since the latter is more dominant, the overall complexity can be approximated as $\sim \mathcal{O}\left(3M\sum_{k=1}^{K-1}(V_k)^3\right)$.

IV. NUMERICAL RESULTS

In this section, we provide numerical results for the proposed scheme and compare its performance with three benchmark schemes for different system parameters. Achievable rates for different schemes are presented by computer simulations. We consider the systems with parameters $M = 25$, $G = 1$, $U = 75$, $R = 25$, $C = 25$, $p_{id} = 21$ dBm, W = 180 kHz, $q_u = 10^5$ bps, $N = 256$, $f_c = 5$ GHz, $D_{in} = 15$ m, $D_{out} = 50$, and $D = 250$ m, $N_0 = -174$ dBm, $P_{max} = 23$ dBm and $P_{min} = -40$ dBm, unless stated otherwise. Although we consider the SINR expression in (7) for RIS assignment in the algorithm, we consider the general SINR expression in (6) while obtaining the numerical results, so that the reflections from non-coherent RIS blocks are considered as well. Achievable rate simulations are obtained by MATLAB software and averaged over 10^6 network realizations. The proposed solution is compared with the following benchmark schemes [22]:

1) The optimal (OPT) PD-NOMA where UEs compute optimal power control based on the readily available CSI, and the maximum and minimum transmit power of UEs are P_{max} and P_{min}, respectively. Throughout the simulations, optimal power weights are obtained by geometric programming solver of the CVX disciplinized convex optimization toolbox [24].

2) Multi-level GF-NOMA (MGF-NOMA) scheme partitions the set of UEs into $R = C$ groups based on their channel gains and divides power control range ($[p_{max} = 23, p_{min} = -40]$ dBm) into $R = C$ levels. MGF-NOMA requires UE partitions with higher channel gain to transmit at higher power levels. For instance, the UE partition consisting of UEs with the highest/lowest channel gains are required to transmit at the highest/lowest power levels.

3) Single level GF-NOMA (SGF-NOMA) scheme requires all UEs transmit at an identical transmit power, p_{id}.
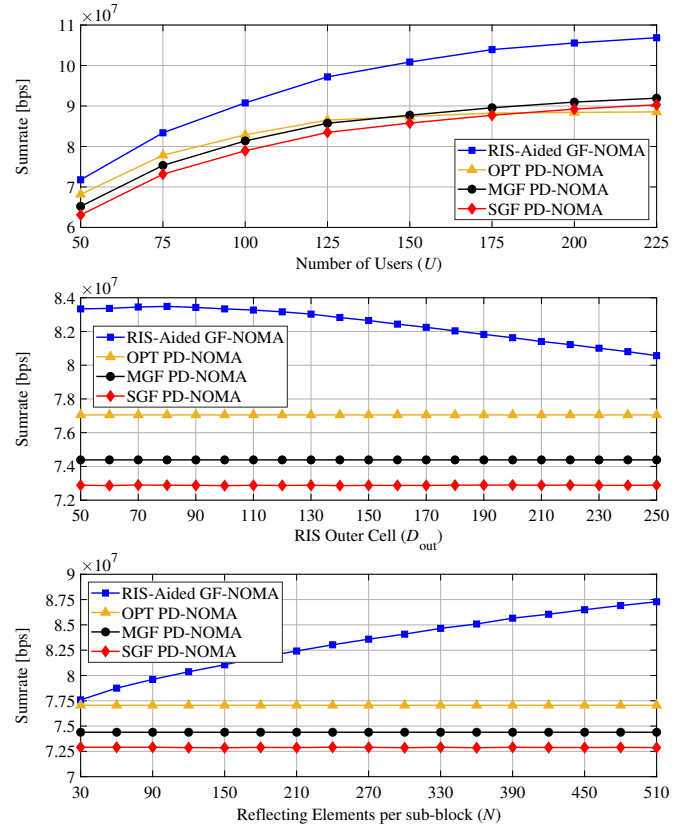
Fig. 2: Network sum rate for different metrics: (a) U, (b) D_{out}, and (c) N.

We refer interested readers to [22] for a more detailed explanation of the benchmark schemes. For the sake of a fair comparison, the proposed schemes uses $p_{id} = 21$ dBm for all UEs, which is the average transmit power of UEs for OPT PD-NOMA. Noting that benchmark schemes do not benefit from RIS, the main difference between compared schemes is the underlying power control approach.

The number of users in a cluster is an important metric that affects the network performance. Fig. 2(a) exhibits the achievable rate of the network for varying U. As seen in Fig. 2(a), the sum rate of the proposed scheme increases with U because the number of users operating in a single resource block increases, resulting in more efficient spectrum usage. The proposed scheme respectively performs 15%, 15% and 18% better than OPT PD-NOMA, MGF-NOMA and SGF-NOMA schemes when $U = 150$. We note that the increase in the cluster size does not have a considerable negative effect on the network performance. The proposed scheme performs better on denser networks, such as where $U = 150$ and the number of users per cluster is 6 and outperforms the benchmark schemes. The performance of the benchmark schemes starts to be saturated after $U = 150$ while the proposed scheme continues to show an upwards trend.

Similar to the number of users in a cluster, the locations of the RISs can also affect the system performance. It is a well-known fact that a basic RIS-assisted system exhibits its maximum performance when the RIS is located near the terminals of the system. Similarly, the proposed design also

gives the best performance when the RISs are close to the BS or users. Fig. 2(b) shows the sum rate of the network for varying D_{out}. The results show that centralized RIS deployment performs better than distributed RIS deployment scenarios because we cannot guarantee that the RISs will be placed close to the users since users are randomly distributed as well. The proposed scheme performs 8%, 12% and 15% better than OPT PD-NOMA, MGF-NOMA and SGF-NOMA schemes, respectively, when $D_{\text{out}} = 80$ m. As D_{out} increases, the sum rate decreases because the RISs gradually become distant from the BS and most of the users. Nevertheless, the proposed scheme still performs 5%, 8% and 11% better than OPT PD-NOMA, MGF-NOMA and SGF-NOMA scheme, respectively, when $D_{\text{out}} = 250$ m. We previously mentioned that an RIS could assist the other users in different clusters, even if its phases are aligned for the dedicated user. This condition also helps further improvement in the sum rate when the RIS placed close to the BS.

RIS size has a considerable impact on the achievable rate of RIS-assisted systems. As shown in Fig. 2(c), the proposed system has nearly the same sum rate with OPT PD-NOMA scheme when $N = 30$, but still performs better than SGF-NOMA scheme by 7%. When $N = 510$, the proposed scheme performs $13/17/20\%$ better than OPT PD-NOMA/MGF-NOMA/SGF-NOMA scheme. The increase in N further increases the performance of the proposed scheme while not affecting the performance of the benchmark schemes since they are not RIS assisted.

V. CONCLUSION

In this paper, an iterative clustering algorithm with a 3D assignment approach has been proposed for an RIS-assisted GF-NOMA system. Through the proposed clustering approach, the network has been found to be able to leverage from the RIS assistance to create received power disparity among NOMA users without the need for complex power control. Moreover, assisting the system with RISs results in better SIC due to the power disparity introduced from the presence of the RISs, leading to improved achievable rates compared with the conventional GF-NOMA with no RIS assistance. Future works can be considered for new schemes that use active RISs instead of the passive ones and assist not only one user in the cluster but all of them, which can come up with some complex optimization problems.

REFERENCES

[1] E. Basar, M. Di Renzo, J. De Rosny, M. Debbah, M.-S. Alouini, and R. Zhang, "Wireless communications through reconfigurable intelligent surfaces," *IEEE Access*, vol. 7, pp. 116 753–116 773, Aug. 2019.

[2] E. Arslan, I. Yildirim, F. Kilinc, and E. Basar, "Over-the-air equalization with reconfigurable intelligent surfaces," *IET Commun.*, 2022. [Online]. Available: https://ietresearch.onlinelibrary.wiley.com/doi/abs/10.1049/cmu2.12425

[3] F. Kilinc, I. Yildirim, and E. Basar, "Physical channel modeling for RIS-empowered wireless networks in sub-6 GHz bands : (invited paper)," in *2021 55th Asilomar Conf. on Signals Syst. Comput.*, Mar. 2021, pp. 704–708.

[4] M.Di Renzo *et al.*, "Reconfigurable intelligent surfaces vs. relaying: Differences, similarities, and performance comparison," *IEEE Open J. Commun. Soc.*, vol. 1, pp. 798–807, Jun. 2020.

[5] Y. Saito, Y. Kishiyama, A. Benjebbour, T. Nakamura, A. Li, and K. Higuchi, "Non-orthogonal multiple access (NOMA) for cellular future radio access," in *2013 IEEE 77th Veh. Technol. Conf.*, Jun. 2013, pp. 1–5.

[6] S. M. R. Islam, N. Avazov, O. A. Dobre, and K.-s. Kwak, "Power-domain non-orthogonal multiple access (NOMA) in 5G systems: Potentials and challenges," *IEEE Commun. Surv.*, vol. 19, no. 2, pp. 721–742, Oct. 2017.

[7] M. B. Shahab, R. Abbas, M. Shirvanimoghaddam, and S. J. Johnson, "Grant-free non-orthogonal multiple access for IoT: A survey," *IEEE Commun. Surv. Tutor.*, vol. 22, no. 3, pp. 1805–1838, May. 2020.

[8] E. Arslan, A. T. Dogukan, and E. Basar, "Index modulation-based flexible non-orthogonal multiple access," *IEEE Wireless Commun. Lett.*, vol. 9, no. 11, pp. 1942–1946, Nov. 2020.

[9] S. Arzykulov, G. Nauryzbayev, A. Celik, and A. M. Eltawil, "Hardware and interference limited cooperative CR-NOMA networks under imperfect SIC and CSI," *IEEE Open J. Commun. Soc.*, vol. 2, pp. 1473–1485, Jun. 2021.

[10] S. Arzykulov, A. Celik, G. Nauryzbayev, and A. M. Eltawil, "UAV-assisted cooperative & cognitive NOMA: Deployment, clustering, and resource allocation," *IEEE Trans. Cogn. Commun.*, vol. 8, no. 1, pp. 263–281, Mar. 2022.

[11] T. Hou, Y. Liu, Z. Song, X. Sun, Y. Chen, and L. Hanzo, "Reconfigurable intelligent surface aided NOMA networks," *IEEE J. Sel. Areas Commun.*, vol. 38, no. 11, pp. 2575–2588, Nov. 2020.

[12] Y. Liu, X. Mu, X. Liu, M. Di Renzo, Z. Ding, and R. Schober, "Reconfigurable intelligent surface-aided multi-user networks: Interplay between NOMA and RIS," *IEEE Wireless Commun.*, vol. 29, no. 2, pp. 169–176, Apr. 2022.

[13] A. Khaleel and E. Basar, "A novel NOMA solution with RIS partitioning," *EEE J. Sel. Top. Signal Process.*, vol. 16, no. 1, pp. 70–81, Jan. 2022.

[14] J. Liu, G. Wu, X. Zhang, S. Fang, and S. Li, "Modeling, analysis, and optimization of grant-free NOMA in massive MTC via stochastic geometry," *IEEE Internet Things J.*, vol. 8, no. 6, pp. 4389–4402, Mar. 2021.

[15] S. Doğan, A. Tusha, and H. Arslan, "NOMA with index modulation for uplink URLLC through grant-free access," *IEEE J. Sel. Topics Signal Process.*, vol. 13, no. 6, pp. 1249–1257, Oct. 2019.

[16] M. Fayaz, W. Yi, Y. Liu, and A. Nallanathan, "Transmit power pool design for grant-free NOMA-IoT networks via deep reinforcement learning," *IEEE Trans. Wireless Commun.*, vol. 20, no. 11, pp. 7626–7641, Nov. 2021.

[17] E. Balevi, F. T. A. Rabee, and R. D. Gitlin, "ALOHA-NOMA for massive machine-to-machine IoT communication," in *2018 IEEE Int. Conf. Commun. (ICC)*, 2018, pp. 1–5.

[18] C. Zhang, Y. Liu, and Z. Ding, "Semi-grant-free NOMA: A stochastic geometry model," *IEEE Trans. Wireless Commun.*, vol. 21, no. 2, pp. 1197–1213, Feb. 2022.

[19] J. Chen, L. Guo, J. Jia, J. Shang, and X. Wang, "Resource allocation for IRS assisted SGF NOMA transmission: A MADRL approach," *IEEE J. Sel. Areas Commun.*, vol. 40, no. 4, pp. 1302–1316, Apr. 2022.

[20] "3GPP TR 38.901 V16.1.0 - Study on channel model for frequencies from 0.5 to 100 GHz," Dec. 2019.

[21] A. Abdallah, A. Celik, M. M. Mansour, and A. M. Eltawil, "Deep learning-based channel estimation for wideband RIS-aided mmWave MIMO system with beam squint," in *Proc. IEEE Int. Conf. Commun. (ICC)*, Seoul, South Korea, 2022, pp. 1269–1275.

[22] A. Celik, "Grant-free NOMA: A low complexity power control through user clustering," April. 2021. [Online]. Available: http://dx.doi.org/10.36227/techrxiv.19688019.v1

[23] K. Pattipati, S. Deb, Y. Bar-Shalom, and R. Washburn, "A new relaxation algorithm and passive sensor data association," *IEEE Trans. Autom. Control*, vol. 37, no. 2, pp. 198–213, Feb. 1992.

[24] M. Grant and S. Boyd, "CVX: Matlab software for disciplined convex programming, version 2.1," http://cvxr.com/cvx, Mar. 2014.